

# Sliding Mode Controller with Sliding Perturbation Observer Based on Gain Optimization Using Genetic Algorithm

Ki Sung You\*

Department of Mechanical and Intelligent Systems  
Engineering  
Pusan National University  
Busan 609-735, Korea  
nedayks@chol.com

Kwon Son\*\*

School of Mechanical Engineering  
Pusan National University  
kson@pusan.ac.kr

Min Cheol Lee\*\*

School of Mechanical Engineering  
Pusan National University  
mclee@pusan.ac.kr

Wan Suk Yoo\*\*

School of Mechanical Engineering  
Pusan National University  
wsyoo@pusan.ac.kr

**Abstract** – This paper proposes a new robust motion control algorithm. The algorithm uses partial state feedback for a class of nonlinear systems with modeling uncertainties and external disturbances. The major contribution is to design a robust observer for the state and the perturbation of the Stewart platform, which is combined with a variable structure controller (VSC). The combination of controller and observer provides the robust routine called sliding mode control with sliding perturbation observer (SMCSPO). The optimal gains of SMCSPO, determined by nominal eigenvalues are easily obtained by genetic algorithm. The proposed fitness function to optimize the gain is defined using the sliding function. The control performance of the proposed algorithm is found to be satisfactory based on the simulation and experiment with Stewart platform.

## 1. INTRODUCTION

The Stewart platform manipulator is a manipulator that has the closed-loop structure with an upper plate of end-effector and a lower plate of base frame [1]. The manipulator has high working accuracy and rigid stiffness compared with a serial one. However, this has such a complex structure that a control performance of the system may not be satisfactory [2].

The major contribution of the design of robust controller introduces the development and design of robust observer for the state and the perturbation, which is integrated into a variable structure controller structure [3]. The combination of controller and observer gives rise to the robust routine called sliding mode control with sliding perturbation observer. The sliding observer is a high performance state estimator well suited for nonlinear uncertain systems with partial state feedback [4].

The sliding function of this observer consists of the estimation error of the available output. The sliding observer does not need a full state feedback in the perturbation estimation and reduces the implementation costs [3].

The combined observer, which can provide better state estimation accuracy, is named sliding perturbation observer (SPO) [5]. The combination of this SPO and

sliding mode controller (SMC) results in a high performance algorithm that is robust against perturbations and utilizes only partial state feedback.

In this paper, a new robust motion control algorithm is proposed using partial state feedback for a class of nonlinear systems with modeling uncertainties and external disturbances. The algorithm is applied to the Stewart platform to evaluate its control performance. Furthermore, the optimal gains of the motion control algorithm are easily obtained by genetic algorithm.

## II. DESIGN OF SLIDING PERTURBATION OBSERVER

This section describes the proposed perturbation observer without considering the closed-loop control. The developed Stewart platform for a vehicle simulator is shown as Fig. 1.

### A. Definition of perturbation

Generally, the governing equation of the j-th actuator with n degree of freedom is defined as

$$\ddot{x}_j = f_j(\mathbf{x}) + \Delta f_j(\mathbf{x}) + \sum_{i=1}^n [(b_{ji}(\mathbf{x}) + \Delta b_{ji}(\mathbf{x}))u_i] + d_j(t) \quad (1)$$

where



Fig. 1 The Stewart platform for a vehicle-driving simulator

$\mathbf{x} \equiv [X_1 \cdots X_n]^T$  : state vector,

$X_j \equiv [x_j \dot{x}_j]^T$  : state variable,

$\Delta f_j(\mathbf{x})$  : uncertainties of nonlinear driving terms,

$\Delta b_{ji}(\mathbf{x})$  : uncertainties of the control gain matrix,

$d_j(t)$  : disturbance,

$u_i$  : control input,

$f_j(\mathbf{x}), b_{ji}(\mathbf{x})$  : continuous functions of state, and

“i”: symbol which represents the element of control gain matrix effected by control input.

In the governing equation, perturbation is defined as the combination of all the uncertainties and nonlinear term in (1).

$$\Psi_j(\mathbf{x}, t) = \Delta f_j(\mathbf{x}) + \sum_{i=1}^n [\Delta b_{ji}(\mathbf{x})u_i] + d_j(t) \quad (2)$$

The control task is to derive the state  $\mathbf{x}$  toward a desired state  $\mathbf{x}_d \equiv [X_{1d} \cdots X_{nd}]^T$  against these perturbations [4]. It is assumed that the perturbations are upper bounded by a known continuous function of the state:

$$\Gamma_j(\mathbf{x}, t) = F_j(\mathbf{x}) + \sum_{i=1}^n |\Phi_{ji}(\mathbf{x})u_i| + D_j(t) > |\Psi_j(t)| \quad (3)$$

where  $F_j > |\Delta f_j|$ ,  $\Phi_{ji} > |\Delta b_{ji}|$ ,  $D_j > |\Delta d_j|$  represent the expected upper bounds of the uncertainties, respectively.

### B. Sliding perturbation observer

Sliding perturbation observer consists of a perturbation observer and sliding observer, in order to be a more effective observer structure. Before integrating SPO into SMC, it is convenient to decouple the control variable. The new control variable used to decouple the control of (1) is defined as

$$f_j(\hat{\mathbf{x}}) + \sum_{i=1}^n b_{ji}(\hat{\mathbf{x}})u_i = \alpha_{3j}\bar{u}_j \quad (4)$$

where  $\hat{\mathbf{x}}$  is the estimated state vector,  $\alpha_{3j}$  is an arbitrary positive number and  $\bar{u}_j$  is the new control variable [5].

Throughout the text, “ $\sim$ ” refers to estimation errors whereas “ $\wedge$ ” symbolizes the estimated quantity. The original control vector of (1) is obtained as

$$\mathbf{u} = \mathbf{B}^{-1} \text{Col}[\alpha_{3j}\bar{u}_j - f_j(\hat{\mathbf{x}})] \quad (5)$$

where  $\mathbf{u} = [u_1 \cdots u_n]^T$  and  $\mathbf{B} = [b_{ji}(\hat{\mathbf{x}})]_{n \times n}$ .

Transformation of (4) allows to simplify the system dynamics. The state representation of the simplified dynamics is given by

$$\dot{x}_{1j} = x_{2j} \quad (6a)$$

$$\dot{x}_{2j} = \alpha_{3j}\bar{u}_j + \Psi_j \quad (6b)$$

$$y_j = x_{1j} \quad (6c)$$

where “j” is the number of hydraulic actuators.

Let  $x_{3j}$  be a new state variable defined as

$$x_{3j} = \alpha_{3j}x_{2j} - \Psi_j / \alpha_{3j}. \quad (7)$$

It is desirable to observe the state variable  $x_{3j}$  and consequently calculate  $\Psi_j$  using this relation instead of estimating it directly[5]. In order to accomplish this, it is assumed that

1. The time derivative of  $\Psi_j$  exists (i.e. there are only continuous perturbations) and is bounded,
2. The spectrum of  $\Psi_j$  lies within a known finite frequency range.

Note that assumption 1 cannot hold at the instant of discontinuities in the perturbation signal (e.g., dry friction at zero velocity point).

The structure of the sliding perturbation observer consists of the perturbation observer and the sliding one. The sliding perturbation observer utilizes only partial state feedback ( $x_{1j}$  in this treatment). Consequently, it is necessary to estimate  $x_{2j}$  in order to obtain the estimated

perturbation  $\hat{\Psi}_j$ . The sliding perturbation observer is better than the general perturbation observer because it can provide an on-line perturbation estimation scheme using only partial state feedback. Also, the estimation accuracy of  $x_{2j}$  improves at least to the order of the perturbation estimation accuracy. At the time derivative of (7), it is assumed that one can select an  $\alpha_{3j}$  high enough so that the term  $\dot{\Psi}_j / \alpha_{3j}$  may be neglected relative to  $\alpha_{3j}\dot{x}_{2j}$ . Based on this assumption with (6) and (7), this new structure can be achieved by writing the observer equation as

$$\dot{\hat{x}}_{1j} = \hat{x}_{2j} - k_{1j} \text{sat}(\tilde{x}_{1j}) - \alpha_{1j}\tilde{x}_{1j} \quad (8a)$$

$$\dot{\hat{x}}_{2j} = \alpha_{3j}\bar{u}_j - k_{2j} \text{sat}(\tilde{x}_{1j}) - \alpha_{2j}\tilde{x}_{1j} + \hat{\Psi}_j \quad (8b)$$

$$\dot{\hat{x}}_{3j} = \alpha_{3j}^2(-\hat{x}_{3j} + \alpha_{3j}\hat{x}_{2j} + \bar{u}_j) \quad (8c)$$

where  $\hat{\Psi}_j$  is derived as

$$\hat{\Psi}_j = \alpha_{3j}(-\hat{x}_{3j} + \alpha_{3j}\hat{x}_{2j}), \quad (9)$$

$k_{1j}$ ,  $k_{2j}$ ,  $\alpha_{1j}$ ,  $\alpha_{2j}$  are positive numbers,

$\tilde{x}_{1j} = \hat{x}_{1j} - x_{1j}$  is the estimation error of the measurable state, and  $\text{sat}(\tilde{x}_{1j})$  is the saturation function for the existence of sliding mode.

### III. COMPOSITION OF CONTROLLER AND GAIN OPTIMIZATION OF SMCSPO

#### A. Design procedure

SMCSPO of robust nonlinear controller becomes strong against perturbations, because of integrating SMC law and SPO scheme. For the system of (6), we define the estimated sliding function as

$$\hat{s}_j = \dot{\hat{e}}_j + c_{j1} \hat{e}_j \quad (10)$$

where  $c_{j1} (> 0)$  is a slope of switching line and  $\hat{e}_j (= \hat{x}_{1j} - x_{1dj})$  is the estimated position tracking error.

$[x_{1dj} \ x_{1dj}]^T$  is the desired states for the motion of the Stewart platform. The control  $\bar{u}_j$  is selected to enforce  $\dot{\hat{s}}_j \hat{s}_j < 0$  outside a prescribed manifold. A desired  $\hat{s}_j$  is selected as

$$\dot{\hat{s}}_j = -K_j \text{sat}(\hat{s}_j) \quad (11)$$

where

$$\text{sat}(\hat{s}_j) = \begin{cases} \hat{s}_j / |\hat{s}_j|, & \text{if } |\hat{s}_j| \geq \varepsilon_{sj} \\ \hat{s}_j / \varepsilon_{sj}, & \text{if } |\hat{s}_j| \leq \varepsilon_{sj} \end{cases} \quad (12)$$

is used due to its desirable anti-chatter properties and  $K_j (> 0)$  is the robust control gain. In this equation,  $\varepsilon_{sj}$  represents the width of boundary layer of SMC, which is different from the boundary layer  $\varepsilon_{oj}$  of SPO.

Using (8), (9), (10), (11), and (12) it is possible to compute  $\hat{s}_j$  as

$$\begin{aligned} \dot{\hat{s}}_j &= \alpha_{3j} \bar{u}_j - [k_{2j} / \varepsilon_{oj} + c_{j1} (k_{1j} / \varepsilon_{oj}) - (k_{1j} / \varepsilon_{oj})^2] \tilde{x}_{1j} \\ &\quad - \ddot{x}_{1dj} + c_{j1} (\hat{x}_{2j} - \dot{x}_{1dj}) + \beta_j \hat{\Psi}_j. \end{aligned} \quad (13)$$

The resulting  $|\hat{s}_j|$ -dynamics including the effects of  $\tilde{x}_{2j}$  is selected as

$$\dot{\hat{s}}_j = -K_j \text{sat}(\hat{s}_j) - (k_{1j} / \varepsilon_{oj}) \tilde{x}_{2j}. \quad (14)$$

In order to enforce (11) when  $\tilde{x}_{2j} = 0$ , a control law is selected as

$$\begin{aligned} \bar{u}_j &= \frac{1}{\alpha_{3j}} \{ -K_j \text{sat}(\hat{s}_j) - (k_{1j} / \varepsilon_{oj}) \tilde{x}_{2j} \\ &\quad + [k_{2j} / \varepsilon_{oj} + c_{j1} (k_{1j} / \varepsilon_{oj}) - (k_{1j} / \varepsilon_{oj})^2] \tilde{x}_{1j} \\ &\quad + \ddot{x}_{1dj} - c_{j1} (\hat{x}_{2j} - \dot{x}_{1dj}) - \beta_j \hat{\Psi}_j \} \end{aligned} \quad (15)$$

where  $\beta_j$  is positive gain of perturbation and  $\beta_j \hat{\Psi}_j$  is upper bounded by a known continuous function of the state (3).

The conditions for the existence of sliding mode are given by

$$\text{sat}(\tilde{x}_{1j}) = \begin{cases} \tilde{x}_{1j} / |\tilde{x}_{1j}|, & \text{if } |\tilde{x}_{1j}| \geq \varepsilon_{oj} \\ \tilde{x}_{1j} / \varepsilon_{oj}, & \text{if } |\tilde{x}_{1j}| \leq \varepsilon_{oj} \end{cases} \quad (16)$$

where  $\varepsilon_{oj}$  is the boundary layer of the sliding perturbation observer.

The observer's sliding mode takes place on the line  $\tilde{x}_{1j} = 0$  of the observer state space  $\tilde{x}_{1j}$  vs.  $\tilde{x}_{2j}$ . Fig. 2 depicts a typical state space trajectory. The conditions for the existence of sliding mode are derived as

$$\tilde{x}_{2j} \leq \alpha_{1j} \tilde{x}_{1j} + k_{1j} \quad (\text{if } \tilde{x}_{1j} > 0) \quad (17a)$$

$$\tilde{x}_{2j} \geq \alpha_{1j} \tilde{x}_{1j} - k_{1j} \quad (\text{if } \tilde{x}_{1j} < 0). \quad (17b)$$

From the sliding condition (17), the state estimation error is bounded by  $|\tilde{x}_{2j}| \leq k_{1j}$ . Therefore, in order to satisfy  $\dot{\hat{s}}_j \hat{s}_j < 0$  outside the manifold  $|\hat{s}_j| \leq \varepsilon_{oj}$ , the robust control gains must be chosen as  $K_j \geq k_{1j}^2 / \varepsilon_{oj}$  from (14).

A systematic general design procedure considering the hardware limitations of the system is described by the fact that the eigenvalues of the characteristic equation of systematic matrix of observer and  $s_j$  dynamics are negative real number. For simplicity, all the desired poles are selected to be the same real valued location  $\lambda = -\lambda_d$  ( $\lambda_d > 0$ ). This leads to the following design solution.

$$\begin{aligned} \frac{k_{1j}}{\varepsilon_{oj}} &= 3\lambda_d, & \frac{k_{2j}}{k_{1j}} &= \lambda_d, \\ \alpha_{3j} &= \sqrt{\frac{\lambda_d}{3}}, & c_{j1} &= K_j / \varepsilon_{oj} = \lambda_d. \end{aligned} \quad (18)$$

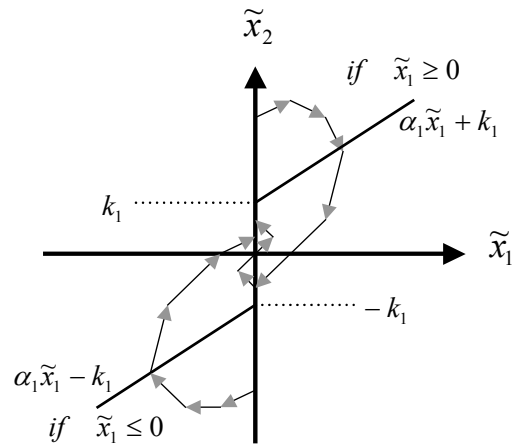


Fig. 2 Observer state space and sliding mode

Physical limitations of the control system define the optimum placement of  $\lambda_d$ . The  $\lambda_d$  is effected by hardware constraints such as sampling frequency, dominant time delay, measurement delay and actuator dynamics.

### B. Gain optimization using genetic algorithm

For evaluating the designed observer performance in the frequency domain, the magnitude plots of  $\tilde{x}_{2j}(p)/\Psi_j(p)$  both for SPO and SO(sliding observer) when perturbation occurs in the system are compared as shown in Fig. 3. SPO clearly yields higher attenuation up to approximately  $\omega/\lambda_d = 0.4$ . This means better estimation accuracy within this normalized frequency. The magnitude plots of  $s_j(p)/\Psi_j(p)$  for SMC and SMCSPO with perturbation are compared as shown in Fig. 4. For higher frequency range of  $\Psi_j$ , both algorithms produce the same magnitude. In the intermediate frequency range, the maximum discrepancy is about 10 dB in favor of SMC. In the lower frequency range, however, SMCSPO performs better than SMC up to a selected frequency equal to  $0.1 \lambda_d$ , which should be set higher than the expected perturbation frequencies so that the attenuation rate of SMCSPO may be larger than that of SMC.

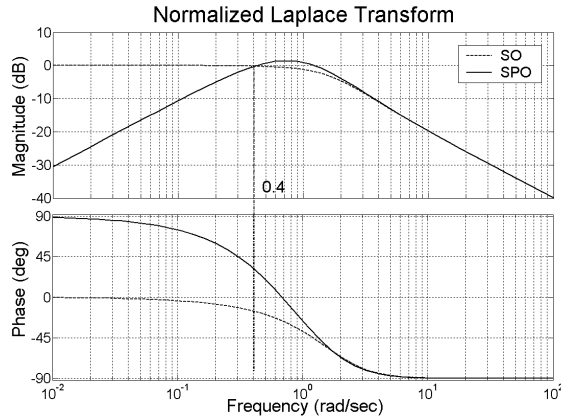


Fig. 3 Bode plots of SPO and SO

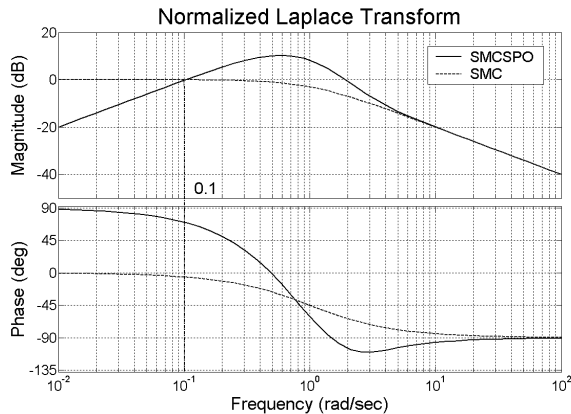


Fig. 4 Bode plots of SMC and SMCSPO

It is important to note that the SMCSPO does not require full state feedback. There is no measurement noise in SMCSPO because chattering is reduced [6, 7]. The selection of optimal placement of  $\lambda_d$  is very hard due to physical limitations of the control system.

In this paper, the genetic algorithm selects the optimal gain  $\lambda_d$ . This algorithm searches the robust control gain using the principles of natural selection. The objective function to optimize the gain consists of the estimated sliding function. The error function and fitness function are given by

$$S_e = \sum_{t=0}^{t_f} \left( \sum_1^n |\hat{s}_i(t)| \right) \quad (19)$$

$$f_{GA} = \frac{W}{1 + S_e} \quad (20)$$

where  $\hat{s}(t)$  is the estimated sliding function for each sampling time and  $W$  is the weighting factor. This function has an effect on optimizing by the velocity and position errors. As the value of error function is reduced, the fitness function is to reach the maximum fitness. The number of generation is 500. The slope of sliding surface is chosen as 21.43.

## IV. SIMULATION AND EXPERIMENT

### A. Modeling of Stewart platform

The dynamic equation of the Stewart platform considering all inertia effect is known to be very difficult to derive. Lebret derived the dynamic equation using the Lagrange method and virtual work principle [1, 8]. This equation is written as

$$M_p(q)\ddot{q} + C_p(q, \dot{q})\dot{q} + G_p(q) = J^T U_p \quad (21)$$

where  $q = [x, y, z, \alpha, \beta, \gamma]$  is the coordinate vector of the upper centroid and  $\alpha, \beta,$  and  $\gamma$  are the rotational angles about the  $x, y,$  and  $z$  axes.  $M_p(q) \in R^{6 \times 6}$  is the inertia matrix,  $C_p(q) \in R^{6 \times 6}$  corresponds to the centrifugal and Coriolis forces matrix,  $G_p(q) \in R^{6 \times 1}$  is the gravity force vector,  $J_p(q) \in R^{6 \times 6}$  is Jacobian matrix, and  $U_p(q) \in R^{6 \times 1}$  is cylinder force vector.

After some algebraic operation ( $\dot{l} = J\dot{q}$ ) and kinematical transformation, (21) can be expressed as

$$\tilde{M}_p(q)\ddot{q} + \tilde{C}_p(q, \dot{q})\dot{q} + \tilde{G}_p(q) = U_p \quad (22)$$

where  $l = [l_1 \dots l_6]$  is the vector of manipulator length

$$\tilde{M}_p(q) = J^{-T}(q)M(q)J^{-1}(q),$$

$$\tilde{C}_p(q, \dot{q})q = J^{-T}(q)M(q)\frac{d}{dt}J^{-1}(q) + J^{-T}(q)C(q, \dot{q})J^{-1}(q),$$

$$\text{and } \tilde{G}_p(q) = J^{-T}(q)G(q).$$

The cylinder dynamic equation is of a high order nonlinear equation. If it is assumed that nonlinear parts act as a disturbance to the model, simple linear dynamics is obtained such as

$$M_A \ddot{l} + C_A \dot{l} + U_P = K_{SV} U_A \quad (23)$$

where  $M_A$  is the summation of equivalent masses of all the translational part in the cylinder,  $C_A$  is the equivalent damping coefficient, and  $K_{SV}$  is a spool constant.

Therefore, the complete nominal dynamic equation of the Stewart platform system is derived as including the manipulator and cylinder dynamics

$$M_T(q) \ddot{l} + C_T(q, \dot{q}) \dot{l} + G_T(q) = K_{SV} U_A \quad (24)$$

where  $M_T = \tilde{M}_p + M_A$ ,  $C_T = \tilde{C}_p + C_A$ ,  $G_T = \tilde{G}_p$ . After separating linear elements and nonlinear ones from (23), this equation can be expressed as

$$M_{TL} \ddot{l} + C_{TL} \dot{l} + F = K_{SV} U_A \quad (25)$$

where  $M_{TL}$  and  $C_{TL}$  is the summation of all linear terms in  $M_T$  and  $C_T$ . The disturbance term is the summation of the nonlinear terms of inertia moments, the Coriolis and centrifugal force, the gravity force, and the friction force. The unknown parameters  $M_{TL}$  and  $C_{TL}$  are estimated by the signal compression method used to obtain an equivalent impulse response [8].

## B. Simulation

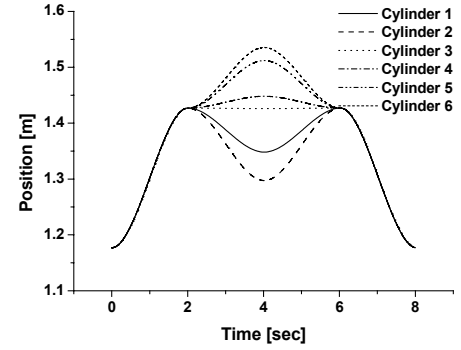
Fig. 5 shows the reference trajectories of position and velocity of the Stewart platform. The motion of the platform is composed of rotational and translational motions. The linear model of hydraulic actuator is derived as

$$\dot{x}_{1j} = x_{2j}, \quad (26a)$$

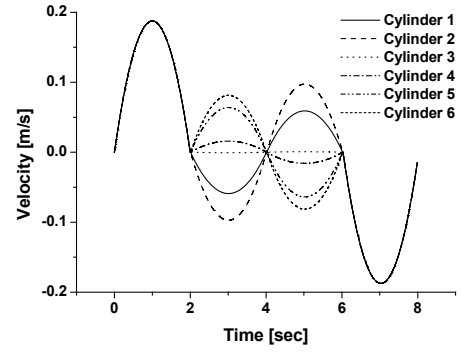
$$\dot{x}_{2j} = -\frac{B_{eq}}{M_{eq}} x_{2j} + \frac{K_{SV}}{M_{eq}} u_j, \quad (26b)$$

where  $K_{SV}$  is the constant of spool,  $[x_1, x_2]$  is the state vector of hydraulic cylinder's rod,  $M_{eq}$  and  $B_{eq}$  is the equivalent viscosity and the equivalent mass, respectively.

Each control loop is designed to complete at 100 Hz since the sampling period is considered as dominant time delay of the closed loop system. Fig. 6 shows the simulated results. They are found to be satisfactory because the position error is less than 2 mm, and the velocity error than 0.01 m/s. The chattering is dramatically reduced as in Fig. 6(a), where seemingly chattering is in fact the sensor noise. Table 1 is the parameter for simulation.

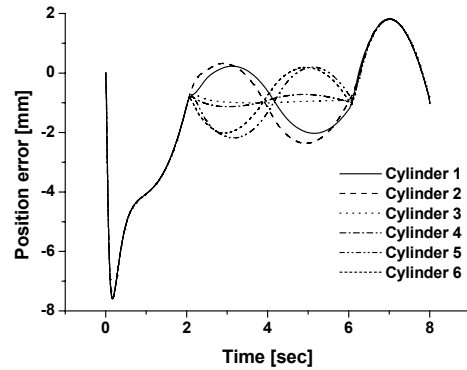


(a) Reference trajectory for position

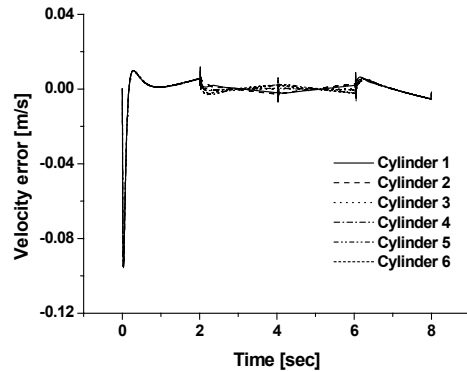


(b) Reference trajectory for velocity

Fig. 5 Reference trajectory



(a) Position tracking error



(b) Velocity tracking error

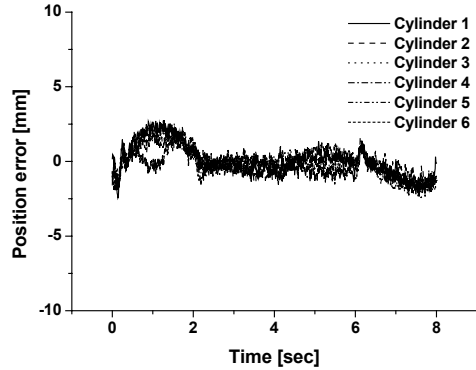
Fig. 6 Results of simulation of sliding mode control with sliding perturbation observer

TABLE 1 PARAMETER SELECTIONS OF SIMULATION

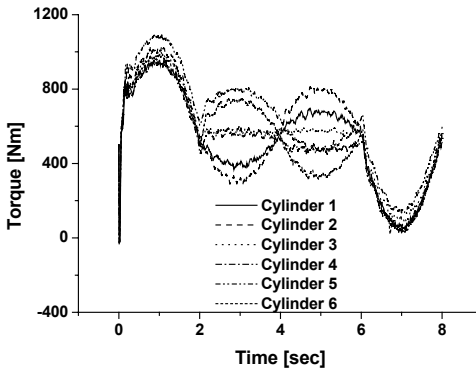
Parameter	Value
$k_{1j} / \varepsilon_{oj}$	60
$k_{2j} / K_{1j}$	20
$\alpha_{3j}$	2.58
$K_j / \varepsilon_{oj}$	20
$c_j$	20
$B_{eq}$	2000
$M_{eq}$	100

### C. Experimental results

In order to evaluate the performance of the proposed control algorithm, we apply the algorithm to Stewart platform. The optimal control gains using genetic algorithm are chosen as  $K_j=20.43$  and  $c_j=20.43$ . The robust gain  $\lambda_d$  is same as the gain of the simulation using the genetic algorithm. In the results of experiment of SMCSPO, Fig. 7 shows that SMCSPO yields better performance with less control activity. The reason for this is the reduction of noise in the velocity feedback. Fig. 7(a) shows that the position tracking errors are converged within 1~2 mm.



(a) Position tracking error



(b) Input torque of system

Fig. 7 Results of experiment of sliding mode control with sliding perturbation observer

### V. CONCLUSIONS

This paper proposed a robust control algorithm for the Stewart platform and described the gain optimization of the control algorithm. The proposed control algorithm can reduce the inherent chattering as estimating the states and compensating a perturbation in accuracy. The sliding perturbation observer is, therefore, proved to be superior to the conventional sliding observer. The optimal gains of SMCSPO are easily obtained by genetic algorithm. The proposed fitness function to optimize the gain is defined using the sliding function. The simulation and experiment results show that SMCSPO can provide reliable tracking performance. This study is noticeable in that the same gains were used both in simulation and experiment. Moreover, the robust control algorithm does not require additional sensor in the system.

### VI. ACKNOWLEDGMENTS

The authors would like to thank the Ministry of Science and Technology of Korea for financial support in the form of grant (M1-0203-00-0017-02J0000-00910) under the NRL (National Research Laboratory).

### VII. REFERENCES

- [1] D. Stewart, "A Platform with Six Degree of Freedom," *Proc. of the Institute of Mechanical Engineering*, Vol. 180, 1966, pp. 317-386.
- [2] H. Hashimoto, K. Maruyama, and F. Harashima, "A Microprocessor-Based Robot Manipulator Control with Sliding Mode," *IEEE Trans. Industrial Electronics*, vol. 34, No. 1, 1987, pp. 11-18.
- [3] J. J. Slotine, J. K. Hedrick, and E. A. Misawa, "On Sliding Observers for Non-Linear Systems." *ASME Journal of Dynamic Systems, Measurement and Control*, Vol. 109, 1987, pp. 245-252.
- [4] H. Elmali and N. Olgac, "Sliding Mode Control with Perturbation Estimation (SMCPE)" *International Journal of Control*, Vol. 56, 1992, pp. 923-941.
- [5] M. J. Terra, H. Elmali, and N. Olgac, "Sliding Mode Control With Sliding Perturbation Observer", *Journal of Dynamic Systems, Measurement, and Control*, Vol. 119, 1997, pp. 657-665.
- [6] M. C. Lee, K. Son, and J. M. Lee, "Improving Tracking Performance of Industrial SCARA Robots Using a New Sliding Mode Control Algorithm," *KSME Int. J.*, vol. 12, No. 5, 1998, pp. 761-772.
- [7] M. C. Lee and N. Aoshima, "Real Time Multi-Input Sliding Mode Control of a Robot Manipulator Based on DSP," *Proc. of SICE*, 1993, pp. 1223-1228.
- [8] M. K. Park and M. C. Lee, "Identification of Motion Platform Using the Signal Compression Method with Pre-processor and Its Application to Sliding Mode Control", *KSME Int. J.*, Vol. 16, No. 11, 2002, pp. 1379-1394.